

# Self-transducible LRS-UNE-L peptide enhances muscle regeneration

Mi-Ock Baek<sup>1</sup>, Hye-Jeong Cho<sup>2</sup>, Do Sik Min<sup>3</sup>, Cheol Soo Choi<sup>4,5,6\*</sup> & Mee-Sup Yoon<sup>1,2,6\*</sup> 

<sup>1</sup>Department of Health Sciences and Technology, GAIHST, Gachon University, Incheon, Republic of Korea; <sup>2</sup>Lee Gil Ya Cancer and Diabetes Institute, Incheon, Republic of Korea; <sup>3</sup>College of Pharmacy, Yonsei University, Incheon, Republic of Korea; <sup>4</sup>Korea Mouse Metabolic Phenotyping Center, Lee Gil Ya Cancer and Diabetes Institute, Gachon University, Incheon, Republic of Korea; <sup>5</sup>Department of Internal Medicine, Gil Medical Center, Gachon University, Incheon, Republic of Korea; <sup>6</sup>Department of Molecular Medicine, Gachon University College of Medicine, Incheon, Republic of Korea

## Abstract

**Background** Muscle regeneration includes proliferation and differentiation of muscle satellite cells, which involves the mammalian target of rapamycin (mTOR). We identified the C-terminal unique attached sequence motif (UNE) domain of leucyl-tRNA synthetase (LRS-UNE-L) as an mTORC1 (mTOR complex1)-activating domain that acts through Vps34 and phospholipase D1 (PLD1) when introduced in the form of a muscle-enhancing peptide.

**Methods** *In vitro* Vps34 lipid kinase assay, phosphatidylinositol 3-phosphate (PI(3)P) measurement, *in vivo* PLD1 assay, and western blot assay were performed in HEK293 cells to test the effect of the LRS-UNE-L on the Vps34-PLD1-mTOR pathway. Adeno-associated virus (AAV)-LRS-UNE-L was transduced in C2C12 cells *in vitro*, in BaCl<sub>2</sub>-injured tibialis anterior (TA) muscles, and in 18-month-old TA muscles to analyse its effect on myogenesis, muscle regeneration, and aged muscle, respectively. The muscle-specific cell-permeable peptide M12 was fused with LRS-UNE-L and tested for cell integration in C2C12 and HEK293 cells using FACS analysis and immunocytochemistry. Finally, M12-LRS-UNE-L was introduced into BaCl<sub>2</sub>-injured TA muscles of 15-week-old *Pld1*<sup>+/+</sup> or *Pld1*<sup>-/-</sup> mice, and its effect was analysed by measurement of cross-sectional area of regenerating muscle fibres.

**Results** The LRS-UNE-L expression restored amino acid-induced S6K1 phosphorylation in LRS knockdown cells in a RagD GTPases-independent manner (421%, *P* = 0.007 vs. LRS knockdown control cells). The LRS-UNE-L domain was directly bound to Vps34; this interaction was accompanied by increases in Vps34 activity (166%, *P* = 0.0352), PI(3)P levels (146%, *P* = 0.0039), and PLD1 activity (228%, *P* = 0.0294) compared with amino acid-treated control cells, but it did not affect autophagic flux. AAV-delivered LRS-UNE-L domain augmented S6K1 phosphorylation (174%, *P* = 0.0013), mRNA levels of myosin heavy chain (MHC) (122%, *P* = 0.0282) and insulin-like growth factor 2 (IGF2) (146%, *P* = 0.008), and myogenic fusion (133%, *P* = 0.0479) in C2C12 myotubes. AAV-LRS-UNE-L increased the size of regenerating muscle fibres in BaCl<sub>2</sub>-injured TA muscles (124%, *P* = 0.0279) (*n* = 9–10), but it did not change the muscle fibre size of TA muscles in old mice. M12-LRS-UNE-L was preferentially delivered into C2C12 cells compared with HEK293 cells and augmented regeneration of BaCl<sub>2</sub>-injured TA muscles in a PLD1-dependent manner (116%, *P* = 0.0022) (*n* = 6).

**Conclusions** Our results provide compelling evidence that M12-LRS-UNE-L could be a muscle-enhancing protein targeting mTOR.

**Keywords** mTOR; Self-transducible peptide; Muscle-enhancing protein; M12-LRS-UNE-L; Muscle regeneration; Muscle differentiation

Received: 7 May 2021; Revised: 13 December 2021; Accepted: 17 January 2022

\*Correspondence to: Mee-Sup Yoon and Cheol Soo Choi, Department of Molecular Medicine, Gachon University College of Medicine, Incheon 21999, Republic of Korea. Email: msyoon@gachon.ac.kr; cschoi@gachon.ac.kr

## Introduction

Skeletal muscle plays an integral role in inter-organ crosstalk for energy and protein metabolism throughout the body, as well as in physical movement and posture.<sup>1</sup> Skeletal muscle also serves as a reservoir of amino acids that can support protein synthesis and energy production.<sup>1</sup> Skeletal muscle restores intact muscle function after injury through its robust regenerative capacity. This regeneration is the result of successful myogenic processes, including muscle stem cell activation and proliferation, cell cycle exit, the fusion of mononucleated myocytes, and the formation of myotubes and myofibres.<sup>2</sup>

The mammalian target of rapamycin (mTOR) governs the anabolic and catabolic signalling that occurs within skeletal muscles, thereby modulating muscle hypertrophy and muscle wastage. mTOR is also a master regulator of skeletal myogenesis via regulation of multiple stages of the myofibre formation process, such as nascent myofibre formation and myofibre growth.<sup>3,4</sup> Rapamycin-resistant (RR) kinase-inactive (KI)-mTOR partially rescues the rapamycin-sensitive myogenic function of mTOR *in vitro* and *in vivo*,<sup>4,5</sup> implying that mTOR controls myogenesis and the early phase of muscle regeneration in both kinase-independent and kinase-dependent manners.<sup>3</sup> Transcription of insulin-like growth factor 2 (IGF-2) through a muscle-specific enhancer is regulated by mTOR through a regulatory mechanism via amino acid-induced Vps34-phospholipase D1 (PLD1) activation.<sup>6</sup> Thus, strategies to enhance mTOR activity in a muscle-specific manner may be important to promote myogenesis, myofibre growth, and maintenance of muscle mass in a diverse muscle-related pathological condition.

Hence, we investigated an attractive and comprehensive method to augment mTOR activity in muscles. We previously reported that leucyl-tRNA synthetase (LRS) activates Vps34-PLD1-mTOR via the C-terminal unique attached sequence motif (UNE) domain of LRS (LRS-UNE-L).<sup>7</sup> In this study, we developed a method to specifically introduce the LRS-UNE-L domain into muscles using M12, a muscle-specific cell-permeable peptide. Thus, we made a muscle-specific self-transducible LRS-UNE-L peptide, which can cross the cell membrane and enter the cell by itself. We proposed that muscle cell-specific delivery of the LRS-UNE-L domain would enhance muscle differentiation *in vivo* and *in vitro* in a mTORC1-dependent manner.

## Methods

Cell culture, cell lysis, immunoprecipitation, western blot analysis, cell viability assay, determination of PLD activity, *in vitro* Vps34 lipid kinase assay, measurement of cellular

phosphatidylinositol 3-phosphate (PI(3)P) levels by ELISA, RNA isolation, quantitative real-time PCR (qRT-PCR), immunofluorescence imaging, and quantitative analysis of myotubes were all performed following standard procedures with detailed information described in the supporting information. Additional information for antibodies, reagents, plasmids, RNAi, and animals appears in the supporting information.

### Purification of MTP-LRS-UNE-L and M12-LRS-UNE-L

The proteins were expressed following protein induction using 0.3 mM isopropyl thiogalactoside (IPTG). After 6 h of induction at 37°C and additional overnight culture at 18°C, bacterial cells were harvested, frozen in lysis buffer [phosphate-buffered saline (PBS), pH 7.4, 1 mM dithiothreitol (DTT), and 10 mg lysozyme], and sonicated at 40 Hz. Lysates were loaded onto glutathione S-transferase (GST)-agarose beads (GE Healthcare, Uppsala, Sweden) and washed with buffer (PBS supplemented with 1 mM DTT, pH 7.4), and proteins were eluted with buffer [50 mM Tris-HCl pH 8.0, 10 mM glutathione reduced (G6529, Sigma-Aldrich)]. After dialysis overnight at 4°C, the eluted proteins were separated from bacterial endotoxins using amicon-100K (UFC810024; Millipore Co., Milford, MA, USA), concentrated with amicon-10K, and subjected to digestion with thrombin (7592; BioVision Incorporated, San Francisco, CA, USA). The aliquots were stored at -80°C. Endotoxin levels were measured using the Pierce LAL Chromogenic Endotoxin Quantitation Kit (88282; Thermo Fisher Scientific, Waltham, MA, USA). The endotoxin levels were determined as follows: MTP-Flag-LRS-UNE-L: 0.0356 Eu/mL; M12-Flag-LRS-UNE-L: 0.0404 Eu/mL; and LRS-UNE-L: 0.0352 Eu/mL.

### Cellular integration of MTP-LRS-UNE-L and M12-LRS-UNE-L

The MTP-LRS-UNE-L or M12-LRS-UNE-L were added to C2C12 myoblasts or HEK293 cells for the specified time in growth media (Dulbecco's Modified Eagle Medium containing 4.5 g/L glucose with 10% foetal bovine serum and 1% penicillin-streptomycin), as indicated in figure legends. For FACS analysis, the cells were washed twice with PBS and then incubated with APC anti-DYKDDK tag (637308; Biolegend, San Diego, CA, USA) for 60 min at room temperature without or with permeabilization of the cell membrane using a Cell Fixation and Permeabilization kit (ab185917; Abcam, Cambridge, UK). After washing with PBS, the cells were analysed by flow cytometry (BD FACS Calibur; BD Biosciences, San Jose, CA, USA), and intracellular levels of MTP-LRS-UNE-L or M12-LRS-UNE-L were analysed. For M12-LRS-UNE-L staining in C2C12 cells, the cells



were washed twice with PBS, fixed in 10% formaldehyde, and permeabilized in 0.1% Triton X-100. After the cells were blocked with 3% bovine serum albumin in PBS, the cells were subjected to intracellular staining with anti-Flag at 4°C overnight. The cells were incubated with Alexa Fluor 488 goat anti-rabbit IgG (A11034, Molecular Probes, Thermo Fisher Scientific). Fluorescent images of cells were captured using a Laser Scanning Confocal Microscope 700 (LSM 700, Carl Zeiss) equipped with an LSM T-PMT camera (Carl Zeiss, LSM 700).

#### AAV-LRS-UNE-L introduction in C2C12 cells and the mouse hindlimb tibialis anterior muscles

For AAV-LRS-UNE-L introduction into C2C12 cells, C2C12 cells were differentiated for 48 h and then transduced with  $4 \times 10^9$  virus particles of AAV-EGFP or AAV-LRS-UNE-L in the differentiation media for 24 h. The cells were incubated in the differentiation media for another 24 h and then subjected to the next procedures described in the figure legends. For AAV-LRS-UNE-L introduction into tibialis anterior (TA) muscles,  $1 \times 10^{11}$  virus particles of AAV-EGFP or AAV-LRS-UNE-L were injected into the mouse hindlimb TA muscle of the EGFP group or UNE-L group of 18-month-old or 10-week-old male mice, respectively. The TA muscles were collected 8 weeks after AAV-EGFP or AAV-LRS-UNE-L introduction in 18-month-old male mice. Fifty microliters of 1.2% (w/v)  $\text{BaCl}_2$  dissolved in saline were injected into the TA muscle of the mice 8 weeks after AAV-EGFP or AAV-LRS-UNE-L introduction in 10-week-old male mice and the TA muscles were collected 5 days after the injury.

#### M12-LRS-UNE-L introduction during $\text{BaCl}_2$ -induced muscle injury

M12-LRS-UNE-L, MTP-LRS-UNE-L, or LRS-UNE-L (22  $\mu\text{M}$ ) protein was co-injected with 50  $\mu\text{L}$  of 1.2% (w/v)  $\text{BaCl}_2$  dissolved in saline in the TA muscles of 15-week-old male *Pld1*<sup>+/+</sup> or *Pld1*<sup>-/-</sup> mice. The injured TA muscles were collected 5 days after injury and subjected to histochemical analysis with haematoxylin and eosin (H&E) staining.

#### Histochemical analysis

The isolated muscles were fixed in 10% formaldehyde solution, embedded in paraffin, serially sectioned, and stained with H&E following standard procedures. Five to ten images of the injured areas were randomly captured using a Motic EasyScan Digital Slide Scanner (Motic Hong Kong Limited, Hong Kong, China). The images were then analysed for cross-sectional area of all centrally nucleated regenerating myofibres using ImageJ software. All analyses were performed by investigators who were blinded to the identities of the samples.

#### Statistical analysis

All values were expressed as mean  $\pm$  standard deviation (SD) of at least three independent experiments. All individual data points are shown in the graphs. All statistical analyses were performed using either the Mann–Whitney *U* test or GraphPad Prism version 9.0 for Microsoft Windows (GraphPad Software, La Jolla, CA, USA). Statistical significance was set at  $P < 0.05$ .

## Results

### UNE-L domain of LRS enhances amino acid-induced Vps34-PLD1-mTORC1 activity

The C-terminal UNE-L domain of LRS is critical for the activity of LRS towards mTORC1.<sup>7</sup> To validate the previously reported role of the LRS-UNE-L domain in the activation of the Vps34/PLD1/mTORC1 axis, we examined whether LRS-UNE-L expression induced the activation of Vps34-PLD1-mTORC1 pathway in cells depleted of LRS by transduction with shRNA for LRS. We first confirmed that the addition of amino acids stimulated Vps34-PLD-mTOR signalling; the extent of stimulation was comparable to that of stimulation with leucine alone (Figure S1A,B,C), which is consistent with a previous report.<sup>7</sup> We utilized the addition of amino acids for the stimulation of Vps34-PLD-mTOR signalling throughout the rest of study. LRS knockdown decreased S6K1 activation, a well-known downstream target of mTORC1, in amino acid stimulation conditions, as previously reported<sup>7</sup> (Figure 1A). The expression of the C-terminal UNE-L domain of LRS (LRS-UNE-L domain) was sufficient to restore amino acid-induced mTORC1 activity, as shown by an increase in S6K1 phosphorylation, in LRS knockdown cells (Figure 1A; 421% increase compared with LRS knockdown control cells). The extent of mTORC1 activation in LRS-UNE-L domain-expressed cells was comparable to that in LRS-wild type (WT-overexpressed cells (Figure 1A). Consistently, LRS-UNE-L expression augmented mTOR phosphorylation at Ser2448 in mTORC1 that was isolated by immunoprecipitation after pre-clearing mTORC2 with anti-riCTOR immunoprecipitation (Figure S2); the extent of Ser2448 phosphorylation was similar to that in LRS-WT-overexpressed cells. However, the expression of either LRS-WT or LRS-UNE-L did not induce mTORC1 activation in the absence of amino acids (Figure 1A). LRS translocates to the lysosome in leucine stimulation, binds to RagD GTPase, and serves as a GTPase activating protein (GAP) of the RagD GTPase.<sup>8,9</sup> BC-LI-0186 is a compound that binds to the RagD-interacting site of LRS and inhibits both lysosomal localization of LRS and mTORC1 activity.<sup>9</sup> Treatment with BC-LI-0186 blocked amino acid-stimulated mTORC1 activity, as shown by a decrease in the phosphorylation of S6K1 at Thr 389 (Figure 1B), as previ-

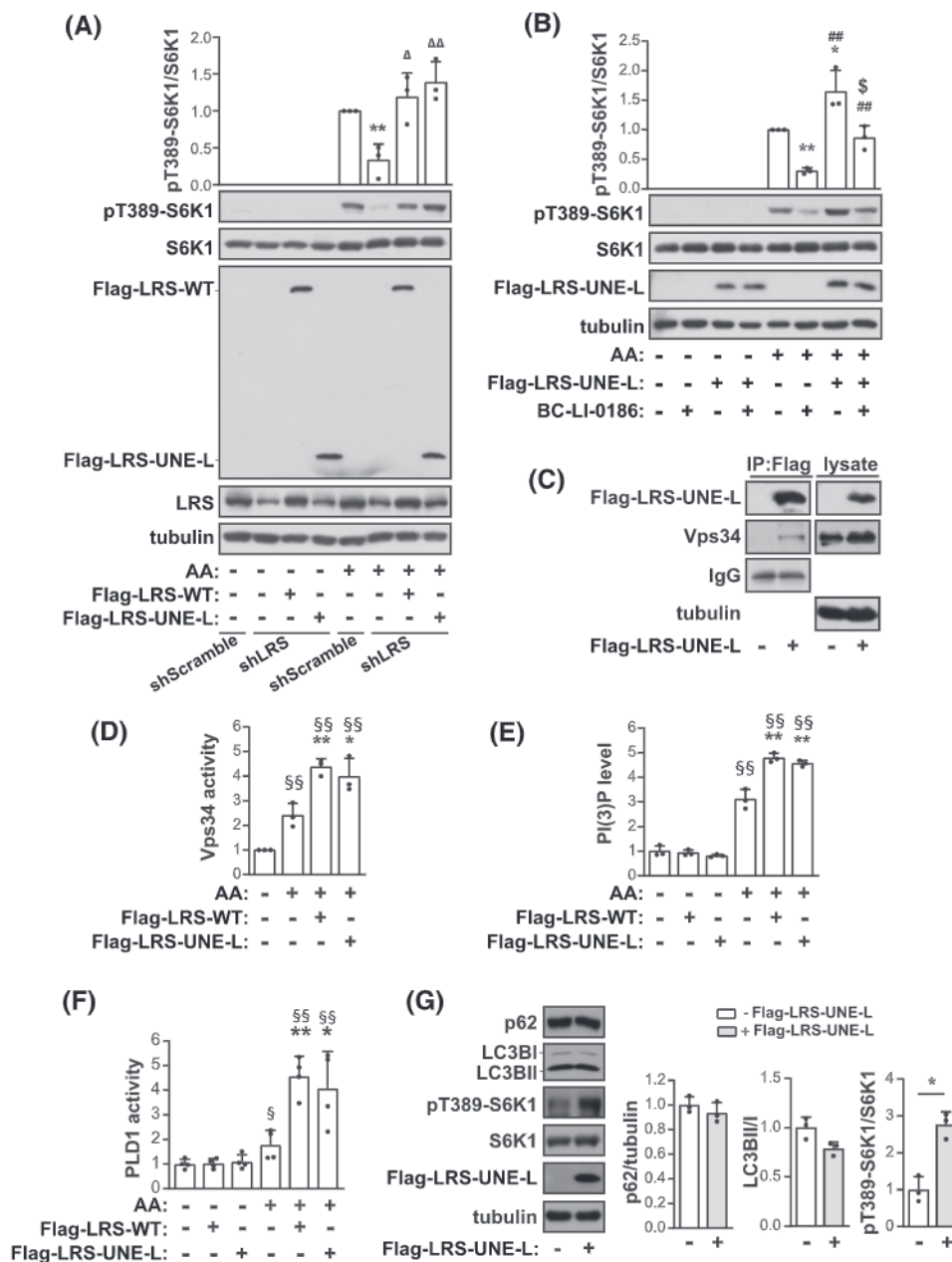


**Figure 1** LRS-UNE-L enhances amino acid-induced Vps34-PLD1-mTORC1 activity. (A) HEK293 cells were transduced with lentivirus expressing shLRS or shScramble (control), selected with puromycin for 3 days, and transfected with Flag-LRS-WT or Flag-LRS-UNE-L. The cells were serum-starved overnight, amino acid-deprived for 2 h, stimulated with amino acids (AA) for 30 min, and then lysed and subjected to western blot analysis ( $n = 3$ ). (B) HEK293 cells were transfected with Flag-LRS-UNE-L, serum-starved overnight, and amino acid-deprived for 2 h. Amino acid stimulation for 30 min was performed in the presence or absence of 30  $\mu$ M BC-LI-0186 before the cells were lysed and subjected to western blot analysis ( $n = 3$ ). (C) HEK293 cells were transfected with Flag-LRS-UNE-L. Anti-Flag immunoprecipitation was conducted, followed by western blot analysis. (D) HEK293 cells were co-transfected with myc-Vps34/V5-Vps15 and Flag-LRS-WT or Flag-LRS-UNE-L. The cells were serum-starved overnight, amino acid-deprived for 2 h, and stimulated with amino acids for 30 min. Anti-myc immunoprecipitates of cell lysates were subjected to *in vitro* kinase assay ( $n = 3$ ). (E) HEK293 cells were transfected with Flag-LRS-WT or Flag-LRS-UNE-L and treated as in (D). PI(3)P levels of lipid extracts were measured by quantitative PI(3)P ELISA assay ( $n = 3$ ). (F) HEK293 cells were co-transfected with HA-PLD1 and Flag-LRS-WT or Flag-LRS-UNE-L and treated as in (D), followed by *in vivo* PLD1 assays ( $n = 4$ ). (G) HEK293 cells were transfected with Flag-LRS-UNE-L, serum-starved overnight, and then subjected to western blot analysis ( $n = 3$ ). All controls were transfected with empty vector. All data shown are the mean  $\pm$  SD or representative blots from 3–5 independent experiments. The intensities of western blots were quantified using ImageJ software (A, B, G). Data were normalized to amino acid-stimulated shScramble transduced cells (A), amino acid-stimulated control (B), amino acid-starved control (D, E, F), or empty vector transfected control (G). \* $P < 0.05$ , \*\* $P < 0.01$  vs. amino acid-stimulated control (A, B, D, E, F);  $\Delta P < 0.05$ ,  $\Delta\Delta P < 0.01$  vs. amino acid-stimulated shLRS-transduced cells (A); ### $P < 0.01$  vs. amino acid + BC-LI-0186 (B); \$ $P < 0.05$  vs. amino acid + Flag-LRS-UNE-L (B); \$ $P < 0.05$ , \$\$ $P < 0.01$  vs. amino acid-starved control (D, E, F); \* $P < 0.05$  vs. empty vector transfected control (G) using GraphPad Prism version 9.0.



ously reported.<sup>9</sup> However, LRS-UNE-L expression partially rescued S6K1 phosphorylation in amino acid stimulation (*Figure 1B*), suggesting that LRS-UNE-L activates mTORC1 activity in a RagD GTPase-independent manner. In line with the effect of the LRS-UNE-L domain on mTORC1 activity, LRS-UNE-L bound to Vps34, suggesting that LRS-UNE-L activates mTOR through direct interaction with Vps34 (*Figure 1C*). This interaction was confirmed and retained in larger LRS fragments containing the LRS-UNE-L domain (e.g. amino acids 1011–1176 and amino acids 1033–1176) but was lost in a larger LRS fragment encompassing amino acids 979–1176 (*Figure S3*). LRS-UNE-L expression increased amino acid-induced Vps34 activity (*Figure 1D*), total cellular PI3P levels (*Figure 1E*), and PLD1 activity (*Figure 1F*) to a similar extent as LRS-WT overexpression. The increases in LRS-UNE-L expressed cells compared with amino acid-treated control cells are 166% in Vps34 activity ( $P = 0.0352$ ), 146% in PI(3)P levels ( $P = 0.0039$ ), and 228% in PLD1 activity ( $P = 0.0294$ ). The overexpression of LRS-WT and LRS-UNE-L did not affect PI(3)P levels and PLD1 activity in absence of amino acids (*Figure 1E,F*). Vps34 functions as a regulator of amino acid signalling in nonautophagic complexes, whereas it regulates autophagy in distinct autophagic complexes.<sup>7</sup> As shown in *Figure 1G*, LRS-UNE-L expression did not affect autophagic flux under serum-starved conditions, as evidenced by the lack of changes in the LC3BII/I ratio and p62 level.

### AAV-LRS-UNE-L augments myogenic differentiation in C2C12 cells

To further examine the biological application of this role of the LRS-UNE-L domain in regulating mTORC1 activity, we investigated the potential function of the LRS-UNE-L domain in myoblast differentiation. The Vps34-PLD1-mTOR axis is a positive regulator of myogenic differentiation by controlling IGF-2 expression.<sup>6</sup> C2C12 myoblasts were induced to differentiate by serum withdrawal for 2 days and then transduced with either AAV-EGFP or AAV-LRS-UNE-L. The high expression of LRS-UNE-L measured in C2C12 myotubes 2 days after AAV-LRS-UNE-L transduction was accompanied by significantly enhanced mRNA expression of IGF-2 and MHC, a late differentiation marker (*Figure 2A*). However, the level of myogenin mRNA, an early differentiation marker, remained unchanged in AAV-LRS-UNE-L-expressing myotubes (*Figure 2A*). In line with this observation, AAV-LRS-UNE-L expression increased the protein level of MHC, and not myogenin, along with augmentation of S6K1 phosphorylation at Thr 389 in C2C12 myotubes (*Figure 2B*), which is consistent with the increase in S6K1 phosphorylation observed in HEK293 cells (*Figure 1A*). In addition, expression of the LRS-UNE-L domain led to a significant augmentation of myogenic differentiation compared with the AAV-EGFP-transduced control, as shown by a signif-

icant increase in the differentiation index, fusion index, and myotube size (*Figure 2C*).

### AAV-LRS-UNE-L enhances muscle regeneration in BaCl<sub>2</sub>-induced muscle injury

To probe the potential effect of the LRS-UNE-L domain in myogenesis *in vivo*, we employed a well-established BaCl<sub>2</sub>-induced muscle injury model. The endogenous LRS mRNA level was enhanced 1–5 days after injury, which was observed together with a remarkable increase in Adgre1 (F4/80)-infiltrating macrophages (*Figure 3A*), suggesting the potential involvement of LRS in *in vivo* myogenesis. AAV-LRS-UNE-L or AAV-EGFP was transduced in the TA muscles of a hindlimb in 10-week-old mice. The expression of LRS-UNE-L was confirmed in the TA muscles of the mice 8 weeks after AAV-LRS-UNE-L transduction (*Figure 3B,C*). After BaCl<sub>2</sub> was injected into the TA muscles of a hindlimb in the mice, the formation of regenerating myofibres was identified by centrally located myonuclei in H&E staining on Day 5 after injury (*Figure 3D*). The number of large regenerating myofibres and the average size of regenerating myofibres was significantly greater in AAV-LRS-UNE-L-transduced TA muscles compared with in AAV-EGFP-transduced TA muscles (*Figure 3E*). Moreover, IGF2 mRNA expression was higher in the TA muscles transduced with AAV-LRS-UNE-L (*Figure 3F*), reflecting an increase in the Vps34-PLD1-mTOR axis.<sup>6</sup> These results are evidence of a positive effect of the LRS-UNE-L construct in muscle regeneration, strongly implying the role of the LRS-UNE-L domain as a positive regulator of muscle regeneration.

### LRS-UNE-L domain does not affect the size of myofibres in aged TA muscles

Next, we examined the effect of LRS-UNE-L expression on the size of myofibres in aged muscles. Transduction with AAV-LRS-UNE-L induced LRS-UNE-L expression in the TA muscles of the hindlimb 8 weeks after AAV-LRS-UNE-L introduction in 18-month-old mice (*Figure 4A,B*). Whereas AAV-transduced LRS-UNE-L expression resulted in a greater number of large myofibres compared with the EGFP control, the average size of the myofibres was not changed significantly (*Figure 4C,D*). IGF2 mRNA expression increased mildly, not significantly, in AAV-LRS-UNE-L transduced old TA muscles (*Figure 4E*). To examine the reason for the weak response to LRS-UNE-L expression in aged TA muscles, we tested the expression levels of the Vps34-PLD1-mTOR axis proteins in young and old muscles. PLD1 mRNA expression was greater in 18-month-old TA muscles,

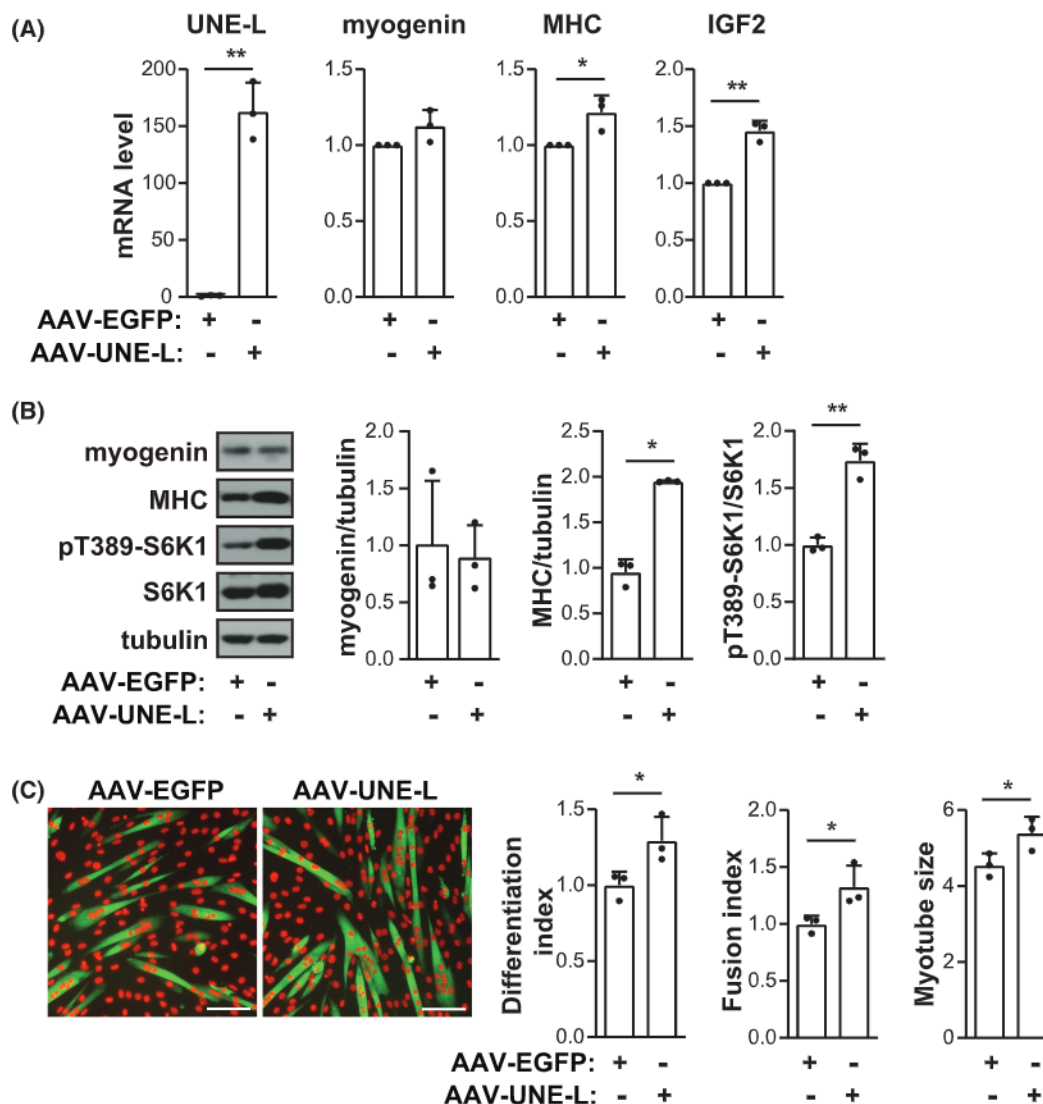


**Figure 2** Adeno-associated virus (AAV)-delivered UNE-L domain of LRS augments myogenic differentiation in C2C12 cells. C2C12 myoblast cells were differentiated for 48 h, transduced with AAV-UNE-L or AAV-EGFP for 24 h, and then incubated in the differentiation media for another 24 h. (A) The cell lysates were analysed using quantitative real-time PCR (qRT-PCR) ( $n = 3$ ). (B) The cell lysates were subjected to western blot analysis ( $n = 3$ ). (C) The cells were stained with MHC (green) and DAPI (red). Scale bar = 50  $\mu$ m. Differentiation index (the number of nuclei in the MHC positive cells/total nuclei), fusion index (the number of nuclei in MHC positive myotubes ( $>2$  myonuclei)/total nuclei), and average myotube size (number of myonuclei/myotube) were quantified ( $n = 3$ ). Data were normalized to AAV-EGFP-transduced cells except myotube size. \* $P < 0.05$  \*\* $P < 0.01$  vs. AAV-EGFP transduced cells by GraphPad Prism version 9.0.

whereas mRNA expression of Vps34 and mTOR were not changed significantly compared with that of 10-week-old TA muscles (Figure 4F). In addition, PLD activity and phosphorylation of 4EBP1 at Ser65, a well-known downstream target of mTORC1, were significantly higher in the gastrocnemii of aged mice (Figure 4G,H), suggesting that the extent of LRS-UNE-L-induced enhancement on PLD1-mTOR activity might not be enough to induce further activation of PLD1-mTOR due to elevated basal activity of PLD1-mTOR in aged muscles.

### Synthesis and characterization of the MTP or M12-conjugated LRS-UNE-L domain

To specifically deliver the LRS-UNE-L domain to muscle cells *in vivo*, we fused the muscle cell-specific permeable peptides MTP or M12 to the LRS-UNE-L domain, respectively (Figure S4A,B). MTP and M12 have been reported as muscle-targeting permeable peptides,<sup>10,11</sup> which led us to use them as a muscle-specific self-delivery vehicle of the



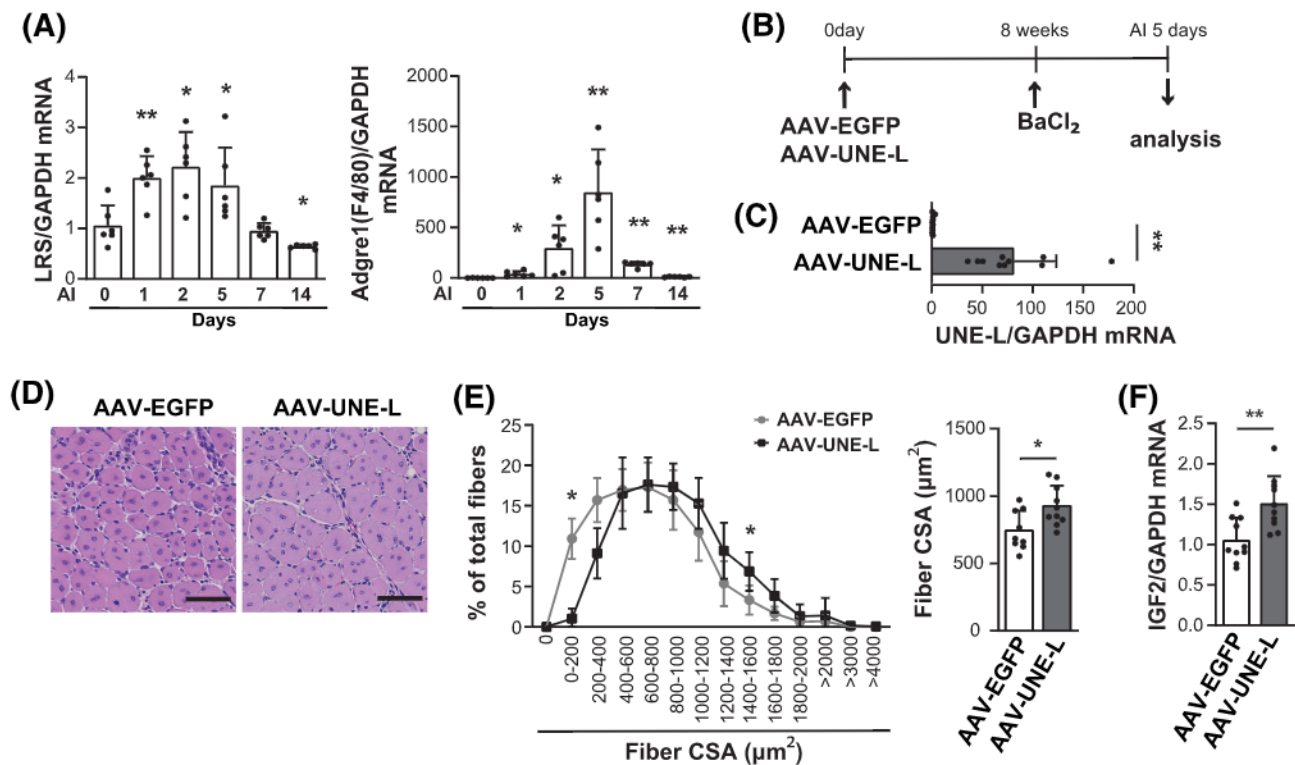


**Figure 3** Adeno-associated virus (AAV)-delivered UNE-L domain of LRS enhances regenerating muscle fibres in BaCl<sub>2</sub>-induced muscle injury. (A) Tibialis anterior (TA) muscles from 10-week-old male mice were injected with BaCl<sub>2</sub> or saline, collected at the indicated days after injury (AI), and subjected to quantitative real-time PCR (qRT-PCR) ( $n = 6$ ). (B) TA muscles from 10-week-old mice were transduced with AAV-EGFP or AAV-UNE-L, injected with BaCl<sub>2</sub> 8 weeks after transduction, and isolated 5 days AI ( $n = 9-10$ ). (C) TA muscles of 10-week-old mice were transduced with AAV-EGFP or AAV-UNE-L, isolated 8 weeks after injection, and subjected to qRT-PCR. (D) Representative haematoxylin and eosin (H&E) images of muscle from (B). Scale bar = 60 μm. (E) The cross-sectional area (CSA) of all centrally nucleated regenerating myofibres in TA muscles from (B) were measured. (F) TA muscles from (B) were subjected to qRT-PCR. \* $P < 0.05$  \*\* $P < 0.01$  vs. AI 0 day (A), or AAV-EGFP group (C, E, F) by Mann-Whitney  $U$  test. All data shown are mean  $\pm$  SD or representative images. Data were normalized to AI 0 day group (A) or AAV-EGFP group (C, F).

LRS-UNE-L domain. GST-MTP-LRS-UNE-L or GST-M12-LRS-UNE-L was expressed in *Escherichia coli* and purified via glutathione chromatography, and GST was removed. Prolonged incubation for 24 h with MTP-LRS-UNE-L or M12-LRS-UNE-L did not affect cell viability *in vitro* (Figure 5A). To determine whether MTP- or M12-LRS-UNE-L could be successfully internalized, we performed flow cytometric analysis of MTP-LRS-UNE-L or M12-LRS-UNE-L in C2C12 cells with or without permeabilization of the cell membrane. MTP-LRS-UNE-L or M12-LRS-UNE-L was readily identified inside C2C12 cells in a concentration-dependent manner with permeabilization of the cell membrane (Figures 5B and S5). MTP-LRS-UNE-L or M12-LRS-UNE-L was detected at a low level inside HEK293 cells compared with C2C12 cells (Figure S6A), suggesting the specificity of MTP-LRS-UNE-L or M12-LRS-UNE-L towards muscle cells. In addition, M12-LRS-UNE-L was not detectable inside C2C12 or HEK293 cells under the condition with non-permeabilization of the cell membrane, whereas MTP-LRS-UNE-L was detected at a low level inside HEK293 cells (Figures 5C and S6B). These results implied that M12-LRS-UNE-L was muscle cell-specifically internalized into C2C12 cells, and that MTP-LRS-UNE-L might, instead, ad-

here to and remain attached to the cell membrane of C2C12 cells. Correspondingly, immunofluorescent staining of C2C12 cells with an anti-Flag confirmed the intracellular delivery of M12-LRS-UNE-L in 1 h (Figure 5D). These results suggest that M12-LRS-UNE-L is a muscle cell-specific self-transducible protein.

### The muscle cell-specific self-transducible peptide M12-conjugated LRS-UNE-L domain augments the size of regenerating fibres in a PLD1-dependent manner

We next assessed the effect of M12-LRS-UNE-L, a muscle cell-specific self-transducible protein, on myogenesis *in vivo*. First, we employed the BaCl<sub>2</sub>-induced injury model in *Pld1*<sup>+/+</sup> and *Pld1*<sup>-/-</sup> mice. The average size of regenerating fibres in TA muscles of *Pld1*<sup>-/-</sup> mice was smaller than that in TA muscles of *Pld1*<sup>+/+</sup> mice 5 days after injury (Figure 6A,B), consistent with previous evidence of a myogenic role for the PLD1-mTORC1 axis *in vivo*.<sup>4,12</sup> Next, BaCl<sub>2</sub> and M12-LRS-

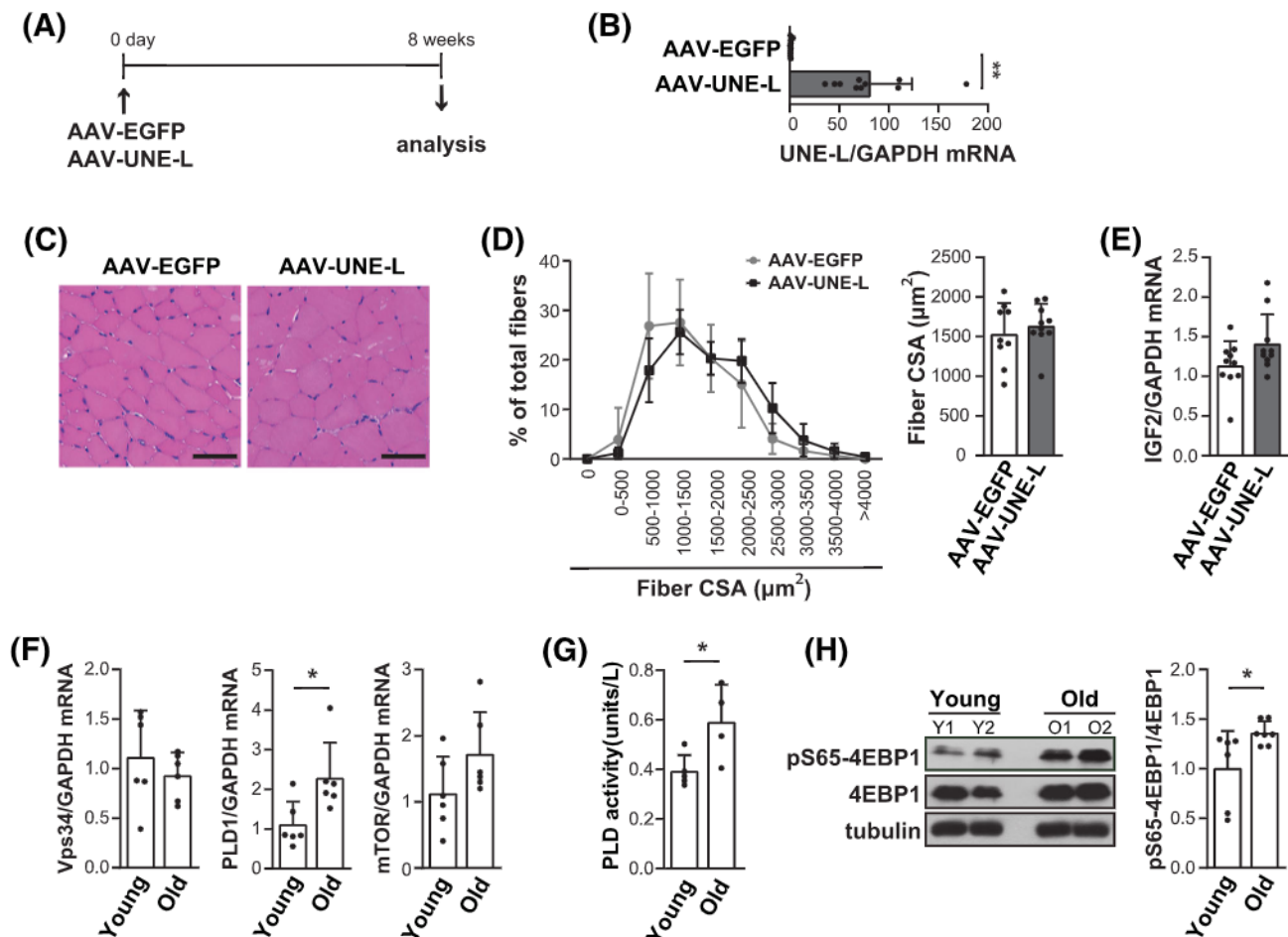


**Figure 4** AAV-delivered UNE-L domain of LRS does not affect muscle fibre size of aged TA muscles. (A) Tibialis anterior (TA) muscles from 18-month-old male mice were injected with AAV-EGFP or AAV-UNE-L and collected 8 weeks after injection ( $n = 9-10$ ). (B) TA muscles from (A) were lysed and analysed by quantitative real-time PCR (qRT-PCR). (C) Representative haematoxylin and eosin (H&E) images of TA muscles from (A). (D) The cross-sectional area (CSA) of TA muscles from (A) were measured. (E) The lysates of TA muscles from (A) were analysed by qRT-PCR. (F) TA muscles from young group (10-week-old) and old group (18-month-old) male mice were isolated, lysed, and subjected to qRT-PCR ( $n = 6$ ). (G, H) Gastrocnemii from young group (10-week-old) and old group (18-month-old) male mice were isolated. (G) The lysates of gastrocnemii were measured for PLD activity according to the manufacturer's procedure ( $n = 4-5$ ). (H) The gastrocnemii were lysed and subjected to western blot analysis ( $n = 6-7$ ). \* $P < 0.05$ , \*\* $P < 0.01$  vs. AAV-EGFP group (B) or young group (F, G, H) by Mann-Whitney  $U$  test. All data shown are mean  $\pm$  SD or representative images. Data were normalized to AAV-EGFP group (B, E) or young group (F, H).

UNE-L or LRS-UNE-L were co-injected into TA muscles of *Pld1*<sup>+/+</sup> and *Pld1*<sup>-/-</sup> mice. As shown in Figure 6C,D, we observed that, on Day 5 after injury, the average cross-sectional area of regenerating fibres in TA muscles of *Pld1*<sup>+/+</sup> mice was significantly larger following the introduction of the muscle-specific M12-LRS-UNE-L protein, compared with the introduction of LRS-UNE-L. On the other hand, injection of MTP-LRS-UNE-L did not affect the size of the regenerating fibres in BaCl<sub>2</sub>-injured TA muscles (Figure S7A, B), consistent with our observation that MTP-LRS-UNE-L does not enter muscle cells (Figures 5B,C). Notably, co-injection of M12-LRS-UNE-L and BaCl<sub>2</sub> in the TA muscles of *Pld1*<sup>-/-</sup> mice did not enhance the average size of regenerating fibres

(Figure 6D). These results provide direct evidence that M12-LRS-UNE-L enhances muscle regeneration through PLD1-mTOR regulation.

## Discussion

The muscle is the central organ of the body's metabolism and maintaining muscle mass is critical for human health. mTORC1 has been identified as a key player in the regulation of muscle mass and function. Here, we report that LRS-UNE-L functions as an activator of mTORC1 signalling in muscle differentiation. Through our efforts to specifically



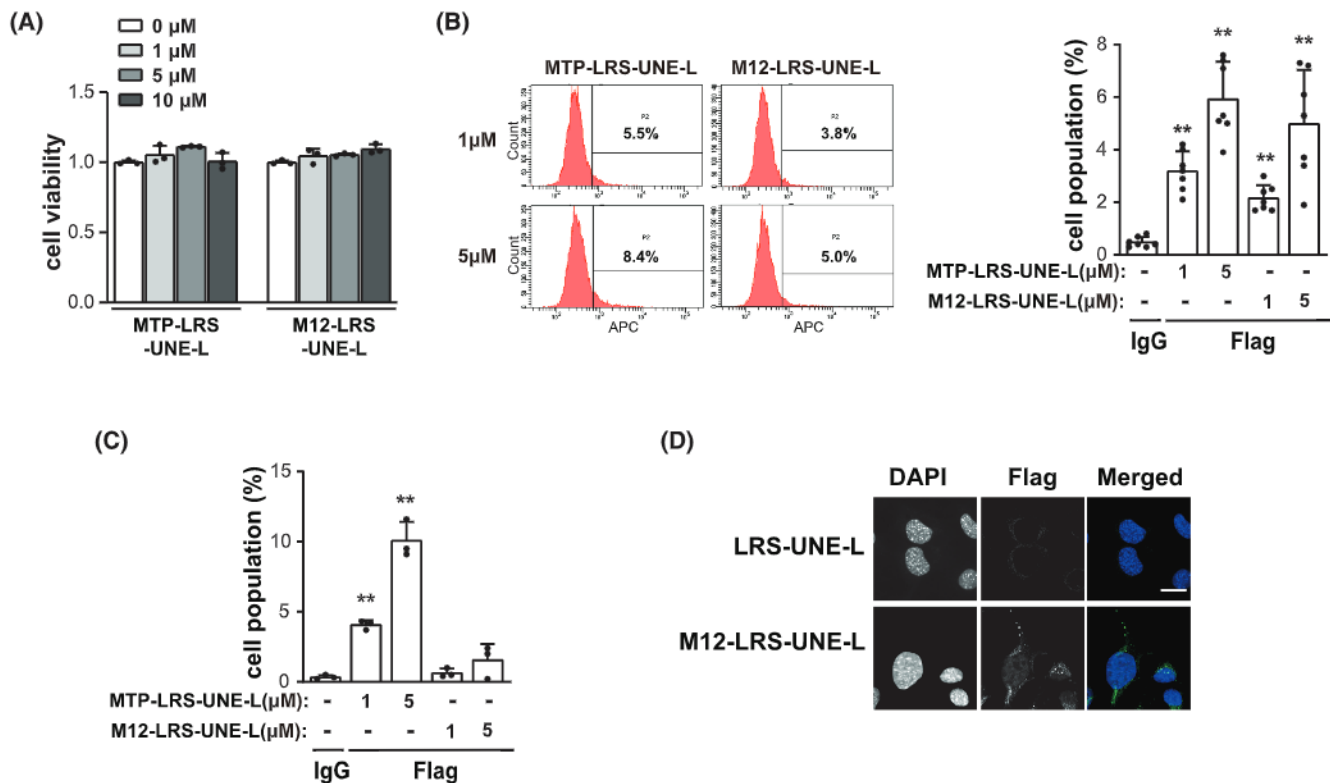


**Figure 5** Characterization of the MTP or M12-conjugated LRS-UNE-L domain. (A) C2C12 myoblast cells were pretreated with or without the indicated concentration of MTP-LRS-UNE-L or M12-LRS-UNE-L for 24 h and subjected to a CCK-8 assay ( $n = 3$ ). (B) MTP-LRS-UNE-L or M12-LRS-UNE-L (1 or 5  $\mu\text{M}$ ) was incubated with C2C12 myoblasts for 1 h. The cells were washed with PBS twice and cultured for an additional 6 h. After the cells were fixed and permeabilized, the intracellular level of MTP-LRS-UNE-L or M12-LRS-UNE-L was quantified by flow cytometry with anti-Flag APC stained cells ( $n = 7$ ). (C) The cells were treated as in (B), fixed, and stained with anti-Flag APC without permeabilization of the cell membrane ( $n = 3$ ). (D) The cells were incubated with 10  $\mu\text{M}$  M12-LRS-UNE-L or LRS-UNE-L for 1 h and washed with PBS twice. The cells were stained with anti-Flag (green) and DAPI (blue) and visualized with a Laser Scanning Confocal Microscope 700. Scale bar = 20  $\mu\text{m}$ . \*\* $P < 0.01$  vs. IgG control using GraphPad Prism version 9.0.

deliver LRS-UNE-L into muscle, we succeeded in activating mTORC1 and enhancing muscle differentiation *in vitro* and *in vivo*.

Our results indicate that LRS-UNE-L augmented muscle differentiation through a noncanonical function of LRS. LRS-UNE-L enhanced the expression of MHC, which is a late marker of myogenesis and is crucial for differentiation as well as muscle fibre formation.<sup>13</sup> LRS-UNE-L did not change the expression of myogenin, an early differentiation marker that acts downstream of both MyoD and Myf5.<sup>14</sup> LRS-UNE-L also increased IGF2 expression, a growth factor in C2C12 differentiation that is regulated by Vps34-PLD1-mTOR following amino acid stimulation.<sup>6</sup>

Contrary to the positive role of LRS-UNE-L in myogenesis in the present study, Son *et al.* showed that LRS inhibits C2C12 differentiation via a process involving leucine binding/sensing that is independent of the protein synthesis rate.<sup>15</sup> LRS binds to RagD GTPase following amino acid stimulation, increasing in insulin receptor substrate (IRS)-1 phosphorylation at Ser307 by mTORC1, subsequent suppression of phosphoino-

sitide 3-kinase (PI3K)-Akt, and inhibition of myogenesis.<sup>8,15</sup> However, this negative role of LRS in myogenesis contradicts the finding that leucine concentration is correlated with C2C12 differentiation<sup>15</sup> and amino acids activate IGF2 transcription during myogenesis.<sup>6</sup> This led us to reason that there is an amino acid-induced positive role of LRS in C2C12 myogenesis that is independent of LRS-RagD GTPase-mTORC1. In support of this, LRS-UNE-L expression augmented the amino acid-induced S6K1 activation in HEK293 cells and this amino-acid induced S6K1 activation remained in the presence of BC-LI-0186 (Figure 1B), a compound that hinders the interaction between LRS and RagD GTPase,<sup>9</sup> indicating a unique RagD-independent regulation of LRS-UNE-L in amino acid-stimulated mTORC1 activation. Furthermore, the region of LRS-WT known to interact with RagD GTPase (amino acids 951–971) is not present in the LRS-UNE-L domain (amino acids 1064–1176),<sup>8</sup> implying that LRS-UNE-L activation of mTORC1 is likely independent of RagD GTPase binding to mTORC1. Nevertheless, LRS-UNE-L cannot activate Vps34-PLD1-mTORC1 in the absence of amino acids, likely be-

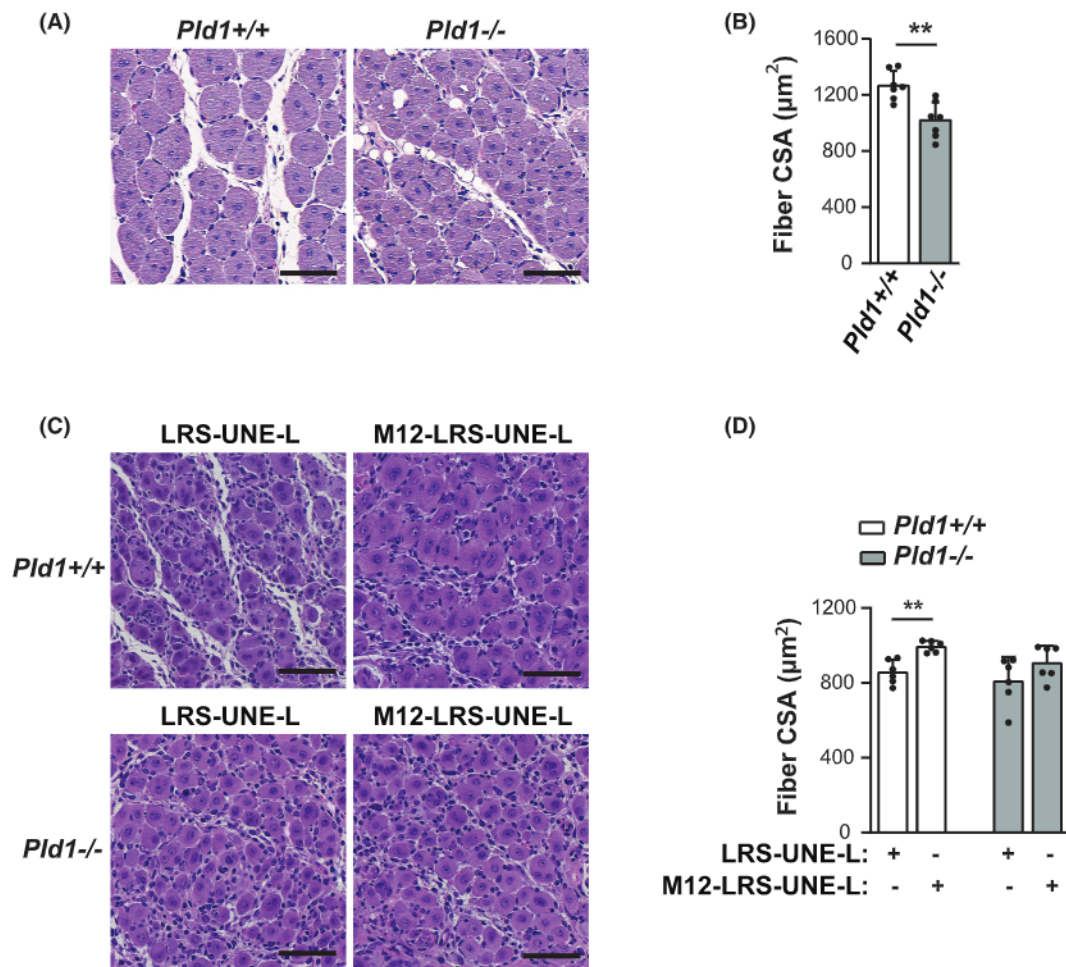


**Figure 6** M12-LRS-UNE-L domain augments muscle regeneration of BaCl<sub>2</sub>-injured TA muscles in a PLD1-dependent manner. (A, B) Tibialis anterior (TA) muscles of 15-week-old male *Pld1*<sup>+/+</sup> (*n* = 7) and *Pld1*<sup>-/-</sup> mice (*n* = 7) were injected with BaCl<sub>2</sub> and isolated on Day 5 after injury. (A) Representative haematoxylin and eosin (H&E) staining images. (B) Myofibre cross-sectional area (CSA) was measured using ImageJ software. Scale bar = 60 μm. (C, D) TA muscles of 15-week-old male *Pld1*<sup>+/+</sup> and *Pld1*<sup>-/-</sup> mice were co-injected with BaCl<sub>2</sub> and LRS-UNE-L or M12-LRS-UNE-L and collected on Day 5 after injury (*n* = 6). (C) Representative H&E staining images. (D) The CSA of regenerating myofibres was measured. \*\**P* < 0.01 compared with *Pld1*<sup>+/+</sup> (A), or *Pld1*<sup>+/+</sup> with LRS-UNE-L (B) by Mann–Whitney *U* test.

cause the Vps34-PLD1 pathway is only one of two required amino acid-sensing pathways upstream of mTORC1 (the other pathway is the RagD pathway). PLD1 translocation via Vps34-PI(3)P occurs independent of Rag-mediated mTORC1 translocation and then PLD1-produced PA activates mTORC1 on the lysosome.<sup>16</sup> Thus, LRS-UNE-L activation of mTORC1, via Vps34 and PLD1, requires the presence of amino acids, likely in order to induce the parallel RagD-mediated mTORC1 translocation on the lysosome.<sup>16,17</sup>

A unique attached sequence motif (UNE), like the UNE-L domain of LRS, was also found in several amino acyl-tRNA synthetases (ARSs).<sup>18</sup> In some cases, these UNE domains are known to interact with other proteins. UNE-I<sub>2</sub>, the second UNE domain of isoleucyl-tRNA synthetase (IRS), mediates its association with the multi-tRNA synthetase complex (MSC).<sup>19</sup> UNE-S, a UNE domain of seryl-tRNA synthetase

(SRS), contains a nuclear localization signal that leads to nuclear translocation of SRS.<sup>20</sup> Until now, the direct interaction of the LRS-UNE-L domain with proteins had not yet been reported. We found that the LRS-UNE-L domain interacted with Vps34 (Figure 1C), providing a mechanistic explanation of UNE-L-induced mTOR activation. This result suggested that the LRS-UNE-L domain could be developed as a practical domain for activating Vps34-PLD-mTOR signalling. However, a cautious approach is required for determining the optimal length of the LRS C-terminal fragment containing LRS-UNE-L for that purpose, because the LRS fragment comprised of amino acids 979–1176 does not appear to interact with Vps34 (Figure S3), nor does the LRS fragment of amino acids 721–1176.<sup>7</sup> We assume that the long C-terminal LRS fragments might form an abnormal structure that conceals the Vps34 interaction motif inside of the LRS-UNE-L domain,



which warrants future investigation. In addition, we cannot completely rule out the possibility that the LRS-UNE-L domain interacts with new regulators other than Vps34 during muscle regeneration to enhance regenerating muscle fibres. Recently, the polypeptide SPAR was reported to bind to Atp6v0a1, leading to stabilization of Ragulator and V-ATPase independent of amino acid stimulation and inhibiting mTORC1 activity in muscle.<sup>21</sup> Whether the LRS-UNE-L domain also functions in myogenesis *in vivo* and *in vitro* through muscle cell-specific protein–protein interactions warrants further investigation.

We utilized M12 and MTP, two muscle-specific peptides, for targeted delivery of LRS-UNE-L to muscle cells. We found that M12-LRS-UNE-L went into the cells, whereas MTP remained at the cell membrane and had a low tendency to enter the cells (Figure 5). Consistent with these findings, we observed that M12-LRS-UNE-L, but not MTP-LRS-UNE-L, enhanced regenerating muscle fibre sizes in BaCl<sub>2</sub>-injured TA muscles (Figures 6 and S7). A previous paper also reported that M12 has more efficient muscle-targeting activity than MTP<sup>11</sup>; M12 conjugated with a phosphorodiamidate morpholino oligomer enhances dystrophin expression more efficiently in muscle cells compared with MTP-conjugated phosphorodiamidate morpholino oligomer with a higher binding affinity to skeletal muscle compared with MTP.<sup>11</sup> The M12 peptide was recently shown to enhance exosome delivery to the muscle by conjugating with CP05, a targeting peptide for exosomes,<sup>22</sup> confirming M12 as a muscle-targeting peptide. However, the muscle protein that binds to M12 is still unknown; further investigation is required to determine the precise mechanism by which M12 targets muscle cells. One such mechanism has already been identified for the laminin  $\alpha 2$  chain peptide A2G80 (VQLRNGFPYFSY), which has a high affinity for  $\alpha$ -dystroglycan that explains its ability to deliver a peptide-gene complex to the muscle.<sup>23</sup>

In the present study, LRS-UNE-L did not enhance the size of aged muscle fibres, whereas it significantly augmented the size of muscle-regenerating fibres in the BaCl<sub>2</sub>-injured TA muscles. We assume that the weak response of the LRS-UNE-L-domain in aged muscles was due to the already high basal activity of PLD1-mTOR in aged muscles. Previous reports showed that mTOR signalling is hyperactive in the skeletal muscles of aged rats and mice.<sup>24,25</sup> Consistently hyperactive mTORC1 in aged muscles increases GDF15 expression and subsequent progressive oxidative stress, resulting in fibre damages and fibre loss.<sup>24</sup> Thus, instead of attempting to increase mTORC1 activity in aged muscles, a new strategy needs to be developed for muscle recovery in this aged context. In the current study, we did not test the effect of LRS-UNE-L on the muscles from female mice. Examination of the effects of LRS-UNE-L on muscle regeneration in female mice is required to conclude that the effects of this peptide are universal.

mTORC1 has been identified as a key player in regulating muscle mass. mTORC1 inhibition by the depletion of a major mTORC1 component, raptor, or overexpression of a mTORC1 suppressor, tuberous sclerosis complex 1 (TSC1), led to muscle atrophy<sup>26,27</sup> and rapamycin, a selective mTOR inhibitor, blocked muscle hypertrophy.<sup>28</sup> The tight interconnection of mTORC1 to the Akt-Forkhead box O (FoxO) pathway or to autophagy induces pathological changes of muscle homeostasis even in mTORC1 activated muscles. The short-term activation of mTORC1 by TSC knockdown in muscles increased muscle fibre size,<sup>29</sup> whereas the sustained activation of mTORC1 by genetic deletion of TSC1 decreased Akt activity, resulting in FoxO activation and an increase in the expression of E3 ubiquitin ligases atrogen and muscle-specific ring finger 1 (MuRF1).<sup>29,30</sup> In addition, the constant activation of mTORC1 in *Tsc1* skeletal muscle-specific knockout mice inhibited ULK1 activity and subsequent autophagy induction, leading to the accumulation of autophagic substrates and the development of a late-onset myopathy.<sup>31</sup> Thus, the duration and extent of mTORC1 activation by M12-LRS-UNE-L need to be thoroughly explored and optimized, specifically with regard to FoxO activation or autophagy inhibition, to maximize the peptide's function as a mTORC1 dependent muscle enhancer. Our initial investigations confirmed that LRS-UNE-L expression did not affect autophagic flux *in vitro* (Figure 1G).

In the present study, we evaluated a functionally important region of LRS, LRS-UNE-L, in muscles and developed it as a muscle-specific self-transducible muscle-enhancing peptide. Its activity was associated with the activation of the Vps34-PLD1-mTORC1 axis, augmentation of myogenesis *in vitro*, and increased muscle regeneration in BaCl<sub>2</sub>-injured muscles. The muscle-specific mTORC1-activating protein, M12-LRS-UNE-L, could be developed as an investigational or therapeutic strategy for a variety of mTORC1-related pathological conditions in muscles.

## Acknowledgements

This work was supported by a National Research Foundation of Korea (NRF) grant funded by the Korean government (Ministry of Science and ICT; NRF-2021R1A2B5B01002047, NRF-2014M3A9D5A01073886), and the Korea Health Technology R&D Project through the Korea Health Industry Development Institute (KHIDI), which was funded by the Ministry for Health and Welfare of Korea (HI17C0426, HR14C0001).

## Conflict of interest

Mi-Ock Baek, Hye-Jeong Cho, Do Sik Min, Cheol Soo Choi, and Mee-Sup Yoon have declared that no competing interest exists.

## Ethics statement

The authors comply with the ethical guidelines for authorship and publishing in the *Journal of Cachexia, Sarcopenia and Muscle*.<sup>32</sup>

## Online supplementary material

Additional supporting information may be found online in the Supporting Information section at the end of the article.

## References

- Argilés JM, Campos N, Lopez-Pedrosa JM, Rueda R, Rodríguez-Mañas L. Skeletal muscle regulates metabolism via interorgan crosstalk: roles in health and disease. *J Am Med Directors Assoc* 2016;**17**:789–796.
- Le Grand F, Rudnicki MA. Skeletal muscle satellite cells and adult myogenesis. *Curr Opin Cell Biol* 2007;**19**:628–633.
- Ge Y, Chen J. Mammalian target of rapamycin (mTOR) signaling network in skeletal myogenesis. *J Biol Chem* 2012;**287**:43928–43935.
- Ge Y, Wu A-L, Warnes C, Liu J, Zhang C, Kawasome H, et al. mTOR regulates skeletal muscle regeneration in vivo through kinase-dependent and kinase-independent mechanisms. *Am J Physiol Cell Physiol* 2009;**297**:C1434–C1444.
- Erbay E, Chen J. The mammalian target of rapamycin regulates C2C12 myogenesis via a kinase-independent mechanism. *J Biol Chem* 2001;**276**:36079–36082.
- Yoon MS, Chen J. Distinct amino acid-sensing mTOR pathways regulate skeletal myogenesis. *Mol Biol Cell* 2013;**24**:3754–3763.
- Yoon MS, Son K, Arauz E, Han JM, Kim S, Chen J. Leucyl-tRNA synthetase activates Vps34 in amino acid-sensing mTORC1 signaling. *Cell Rep* 2016;**16**:1510–1517.
- Han JM, Jeong SJ, Park MC, Kim G, Kwon NH, Kim HK, et al. Leucyl-tRNA synthetase is an intracellular leucine sensor for the mTORC1-signaling pathway. *Cell* 2012;**149**:410–424.
- Kim JH, Lee C, Lee M, Wang H, Kim K, Park SJ, et al. Control of leucine-dependent mTORC1 pathway through chemical intervention of leucyl-tRNA synthetase and RagD interaction. *Nat Commun* 2017;**8**:732.
- Yu CY, Yuan Z, Cao Z, Wang B, Qiao C, Li J, et al. A muscle-targeting peptide displayed on AAV2 improves muscle tropism on systemic delivery. *Gene Ther* 2009;**16**:953–962.
- Gao X, Zhao J, Han G, Zhang Y, Dong X, Cao L, et al. Effective dystrophin restoration by a novel muscle-homing peptide-morpholino conjugate in dystrophin-deficient mdx mice. *Mol Ther: the journal of the American Society of Gene Therapy* 2014;**22**:1333–1341.
- Teng S, Stegner D, Chen Q, Hongu T, Hasegawa H, Chen L, et al. Phospholipase D1 facilitates second-phase myoblast fusion and skeletal muscle regeneration. *Mol Biol Cell* 2015;**26**:506–517.
- Miller JB. Myogenic programs of mouse muscle cell lines: expression of myosin heavy chain isoforms, MyoD1, and myogenin. *J Cell Biol* 1990;**111**:1149–1159.
- Ganassi M, Badodi S, Wanders K, Zammit PS, Hughes SM. Myogenin is an essential regulator of adult myofibre growth and muscle stem cell homeostasis. *Elife* 2020;**9**.
- Son K, You JS, Yoon MS, Dai C, Kim JH, Khanna N, et al. Nontranslational function of leucyl-tRNA synthetase regulates myogenic differentiation and skeletal muscle regeneration. *J Clin Invest* 2019;**129**:2088–2093.
- Yoon MS, Du G, Backer JM, Frohman MA, Chen J. Class III PI-3-kinase activates phospholipase D in an amino acid-sensing mTORC1 pathway. *J Cell Biol* 2011;**195**:435–447.
- Fang Y, Vilella-Bach M, Bachmann R, Flanigan A, Chen J. Phosphatidic acid-mediated mitogenic activation of mTOR signaling. *Science* 2001;**294**:1942–1945.
- Kwon NH, Fox PL, Kim S. Aminoacyl-tRNA synthetases as therapeutic targets. *Nat Rev Drug Discov* 2019;**18**:629–650.
- Guo M, Yang XL. Architecture and metamorphosis. *Top Curr Chem* 2014;**344**:89–118.
- Xu X, Shi Y, Zhang HM, Swindell EC, Marshall AG, Guo M, et al. Unique domain appended to vertebrate tRNA synthetase is essential for vascular development. *Nat Commun* 2012;**3**:681.
- Matsumoto A, Pasut A, Matsumoto M, Yamashita R, Fung J, Monteleone E, et al. Pandolfi PP: mTORC1 and muscle regeneration are regulated by the LINC00961-encoded SPAR polypeptide. *Nature* 2017;**541**:228–232.
- Gao X, Ran N, Dong X, Zuo B, Yang R, Zhou Q, Moulton HM, Seow Y, Yin H: Anchor peptide captures, targets, and loads exosomes of diverse origins for diagnostics and therapy. *Sci Transl Med* 2018;**10**:eaat0195.
- Nirasawa K, Hamada K, Naraki Y, Kikkawa Y, Sasaki E, Endo-Takahashi Y, et al. Development of A2G80 peptide-gene complex for targeted delivery to muscle cells. *J Control Release* 2021;**329**:988–996.
- Tang H, Inoki K, Brooks SV, Okazawa H, Lee M, Wang J, et al. mTORC1 underlies age-related muscle fiber damage and loss by inducing oxidative stress and catabolism. *Aging Cell* 2019;**18**:e12943.
- Sandri M, Barberi L, Bijlsma AY, Blaauw B, Dyar KA, Milan G, et al. Signalling pathways regulating muscle mass in ageing skeletal muscle. The role of the IGF1-Akt-mTOR-FoxO pathway. *Biogerontology* 2013;**14**(3):303–323.
- Bentzinger CF, Romanino K, Cloetta D, Lin S, Mascarenhas JB, Oliveri F, et al. Skeletal muscle-specific ablation of raptor, but not of rictor, causes metabolic changes and results in muscle dystrophy. *Cell Metab* 2008;**8**:411–424.
- Wan M, Wu X, Guan KL, Han M, Zhuang Y, Xu T. Muscle atrophy in transgenic mice expressing a human TSC1 transgene. *FEBS Lett* 2006;**580**:5621–5627.
- Bodine SC, Stitt TN, Gonzalez M, Kline WO, Stover GL, Bauerlein R, et al. Akt/mTOR pathway is a crucial regulator of skeletal muscle hypertrophy and can prevent muscle atrophy in vivo. *Nat Cell Biol* 2001;**3**:1014–1019.
- Bentzinger CF, Lin S, Romanino K, Castets P, Guridi M, Summermatter S, et al. Differential response of skeletal muscles to mTORC1 signaling during atrophy and hypertrophy. *Skeletal Muscle* 2013;**3**:6.
- Tang H, Inoki K, Lee M, Wright E, Khuong A, Khuong A, et al. mTORC1 promotes denervation-induced muscle atrophy through a mechanism involving the activation of FoxO and E3 ubiquitin ligases. *Sci Signal* 2014;**7**:ra18.
- Castets P, Rüegg MA. mTORC1 determines autophagy through ULK1 regulation in skeletal muscle. *Autophagy* 2013;**9**:1435–1437.
- von Haehling S, Morley JE, Coats AJS, Anker SD. Ethical guidelines for publishing in the *Journal of Cachexia, Sarcopenia and Muscle*: update 2021. *J Cachexia Sarcopenia Muscle* 2021;**12**:2259–2261.